Journal of Visualized Experiments

Solution Blow Spinning of Polymeric Nano-Composite Fibers for Personal Protective Equipment

--Manuscript Draft--

Article Type:	Invited Methods Article - JoVE Produced Video
Manuscript Number:	JoVE62283R1
Full Title:	Solution Blow Spinning of Polymeric Nano-Composite Fibers for Personal Protective Equipment
Corresponding Author:	Amanda Forster National Institute of Standards and Technology Gaithersburg, MD UNITED STATES
Corresponding Author's Institution:	National Institute of Standards and Technology
Corresponding Author E-Mail:	amanda.forster@nist.gov
Order of Authors:	Zois Tsinas
	Ran Tao
	Amanda Forster
Additional Information:	
Question	**Response**
Please indicate whether this article will be Standard Access or Open Access.	Standard Access (US$2,400)
Please specify the section of the submitted manuscript.	Engineering
Please indicate the **city, state/province, and country** where this article will be **filmed**. Please do not use abbreviations.	Gaithersburg, MD USA
Please confirm that you have read and agree to the terms and conditions of the author license agreement that applies below:	I agree to the Author License Agreement
Please provide any comments to the journal here.	
Please indicate whether this article will be Standard Access or Open Access.	Standard Access ($1400)

TITLE:
Solution Blow Spinning of Polymeric Nano-Composite Fibers for Personal Protective Equipment

AUTHORS AND AFFILIATIONS:
Zois Tsinas[1,2], Ran Tao[1,3], Amanda L. Forster[1]

[1]Material Measurement Laboratory, National Institute of Standards and Technology, Gaithersburg, MD, USA
[2]Theiss Research, La Jolla, CA, USA
[3]Department of Chemical Engineering, Texas Tech University, Lubbock, TX, USA

Email addresses of co-authors:
Zois Tsinas (zois.tsinas@nist.gov)
Ran Tao (ran.tao@nist.gov)

Corresponding author:
Amanda L. Forster (amanda.forster@nist.gov)

KEYWORDS:
Solution Blow Spinning (SBS), polymeric fibers, fiber nanocomposites, Scanning Electron Microscopy (SEM), poly(styrene-butadiene-styrene), iron oxide (Fe_3O_4) nanoparticles

SUMMARY:
The primary goal of this study is to describe a protocol to prepare polymeric fiber mats with consistent morphology via solution blow spinning (SBS). We aim to use SBS to develop novel, tunable, flexible polymeric fiber nanocomposites for various applications, including protective materials, by incorporating nanoparticles in a polymer-elastomer matrix.

ABSTRACT:
Light-weight, protective armor systems typically consist of high modulus (>10^9 MPa) and high-strength polymeric fibers held in place with an elastic resin material (binder) to form a non-woven, unidirectional laminate. While significant efforts have focused on improving the mechanical properties of the high-strength fibers, little work has been undertaken to improve the properties of the binder materials. To improve the performance of these elastomeric polymer binders, a relatively new and simple fabrication process, known as solution blow spinning, was used. This technique is capable of producing sheets or webs of fibers with average diameters ranging from the nanoscale to the microscale. To achieve this, a solution blow spinning (SBS) apparatus has been designed and built in the laboratory to fabricate non-woven fiber mats from polymer elastomer solutions.

In this study, a commonly used binder material, a styrene-butadiene-styrene block-co-polymer dissolved in tetrahydrofuran, was used to produce nanocomposite fiber mats by adding metallic nanoparticles (NPs), such as iron oxide NPs, that were encapsulated with polymer and thus incorporated in the fibers formed via the SBS process. The protocol described in this work will

discuss the effects of the various critical parameters involved in the SBS process, including the polymer molar mass, the selection of the thermodynamically appropriate solvent, the polymer concentration in solution, and the carrier gas pressure to assist others in performing similar experiments, as well as provide guidance to optimize the configuration of the experimental setup. The structural integrity and morphology of the resultant non-woven fiber mats were examined using scanning electron microscopy (SEM) and elemental X-ray analysis via energy-dispersive X-ray spectroscopy (EDS). The goal of this study is to evaluate the effects of the various experimental parameters and material selections to optimize the structure and morphology of the SBS fiber mats.

INTRODUCTION:

Many light-weight, ballistic, protective armor systems are currently constructed using high-modulus and high-strength polymeric fibers, such as oriented, ultra-high molar mass polyethylene fibers or aramids, which provide outstanding ballistic resistance[1,2]. These fibers are used in combination with an elastic resin material (binder) that can penetrate to the filament level and secure the fibers in a 0°/90° configuration to form a non-woven, unidirectional laminate. The percentage of the polymer elastomer resin (binder) should not exceed 13% of the total weight of the unidirectional laminate to maintain the structural integrity and antiballistic properties of the laminate structure[3,4]. The binder is a very important component of the armor as it keeps the high-strength fibers properly oriented and tightly packed within each laminate layer[3]. Elastomer materials commonly used as binders in body armor applications have very low tensile modulus (*e.g.*, ~17.2 MPa at ~23 °C), low glass transition temperature (preferably below -50 °C), very high elongation at break (as high as 300%) and must demonstrate excellent adhesive properties[5].

To improve the performance of these polymer elastomers, SBS was used to create fibrous elastomer materials that can be used as binders in body armor applications. SBS is a relatively new, versatile technique allowing the use of different polymer/solvent systems and the creation of different end products[6-13]. This simple process involves the rapid (10x the rate of electrospinning) deposition of conformal fibers onto both planar and nonplanar substrates to fabricate sheets or webs of fibers of both the nano and micro scale diameters[14-18]. SBS materials have numerous applications in medical products, air filters, protective equipment, sensors, optical electronics, and catalysts[14,19,20]. Developing small diameter fibers can drastically increase the surface area to volume ratio, which is very important for several applications, especially in the personal protective equipment field. The diameter and morphology of the fibers generated by SBS depends on the molar mass of the polymer, polymer concentration in the solution, viscosity of the solution, polymer solution flow rate, gas pressure, working distance, and diameter of the spray nozzle[14,15,17].

An important characteristic of the SBS apparatus is the spray nozzle consisting of an inner and a concentric outer nozzle. The polymer dissolved in a volatile solvent is pumped through the inner nozzle while a pressurized gas flows through the outer nozzle. The high-velocity gas exiting the outer nozzle induces shearing of the polymer solution flowing through the inner nozzle. This forces the solution to form a conical shape when exiting the spray nozzle. When the surface

tension at the tip of the cone is overcome, a fine stream of polymer solution is ejected, and the solvent rapidly evaporates causing polymer strands to coalesce and deposit as polymer fibers. The formation of a fibrous structure, as solvent evaporates, strongly depends on the polymer molar mass and the solution concentration. Fibers are formed by chain entanglement, when polymer chains in solution begin to overlap at a concentration known as the critical overlap concentration (c*). Therefore, it is necessary to work with polymer solutions above the c* of the polymer/solvent system selected. An easy strategy to attain this is to choose polymers with relatively high molar mass. However, polymers with higher molar mass have increased polymer relaxation times, which is directly related to an increase in the formation of fibrous structures, as described in the literature[21]. As many of the parameters used in SBS are strongly correlated, the goal of this work is to provide guidance to develop tunable, and flexible polymeric fiber nanocomposites to be used as alternatives for typical binder materials found in body armor applications by incorporating nanoparticles in the fibrous polymer-elastomer matrix.

PROTOCOL:

NOTE: Details related to the equipment, instrumentation, and chemicals used in this section can be found in the **Table of Materials**. This entire protocol should first be reviewed and approved by the institutional safety department/personnel to ensure procedures and processes specific to the institution are adhered to.

1. Preparation of polymer solution using the appropriate solvent

NOTE: Consult manufacturer/supplier safety data sheets and the institution's safety department/personnel regarding proper personal protective equipment (PPE) to use with each chemical/material.

1.1. Use a clean small laboratory spatula, and transfer the desired amount (*e.g.*, ~2 g) of dry polymer (poly(styrene-butadiene-styrene)) into a clean, empty, 20 mL borosilicate glass vial. Seal the vial, and store under ambient laboratory conditions.

NOTE: The selected concentration for poly(styrene-butadiene-styrene) in tetrahydrofuran (THF) was approximately 200 mg/mL. This concentration is used as an example throughout this protocol; the optimal concentration will depend on the polymer/solvent system used.

1.2. Transfer the borosilicate glass vial containing the polymer sample into a chemical fume hood, and pipette 10 mL ± 0.1 mL of the desired solvent, in this case THF, into the vial to achieve the desired concentration of nominally 200 mg/mL.

1.3. Seal the solvent (THF) container, and transfer it to the storage cabinet. Cap the borosilicate glass vial containing the polymer/solvent sample with the provided lid, and carefully mount it on a mixer/rotator.

1.4. Agitate the mixture at room temperature using a rotator at 70 rpm until the polymer fully

dissolves in the solvent.

NOTE: The solution appears clear and transparent after approximately 60 min, denoting complete polymer dissolution.

1.5. Transfer the solution into a dissolved gas analysis (DGA) borosilicate glass syringe for SBS.

NOTE: Polymer solutions can be stored and used for up to 72 h, provided that the borosilicate glass vial is securely capped, and the opening is wrapped using a paraffin wax film. However, the solutions must be agitated again before performing SBS.

2. Determination of critical overlap polymer concentration by viscosity measurement

NOTE: This step is provided here to determine the critical overlap polymer concentration, which is an important parameter that affects the overall fiber quality and morphology after SBS. See the representative results and discussion sections for details.

2.1. Prepare eight nominal concentrations (1 mg/mL, 3 mg/mL, 5 mg/mL, 10 mg/mL, 20 mg/mL, 30 mg/mL, 40 mg/mL, 50 mg/mL) of the polymer solution in THF with an approximate volume of 10 mL. Follow the same procedure as in steps 1.1 and 1.2 to prepare the solutions.

2.2. Prepare the rheometer for measurements.

NOTE: Routine calibration and verification checks for torque, normal force, and phase angle should be performed on the rheometer prior to the following setup procedure.

2.2.1. Install the environmental control device on the rheometer for temperature control.

2.2.2. Install the rheometer geometry, *i.e.*, recessed concentric cylinders on the rheometer. First, insert and install the lower geometry (cup) into the environmental control device and then the upper geometry (bob) on the transducer shaft.

2.2.3. Tare normal force and torque using the instrument touch screen. Zero the geometry gap using the gap control function of the rheometer software. Raise the stage to provide enough space for sample loading.

2.3. Load the polymer solution into the cup using a high-quality, disposable borosilicate glass pipette (minimum sample volume for the geometry ~7 mL). Set the gap to the operating gap (3.6 mm) for the measurement.

2.4. Perform a shear rate sweep test from about 10 s^{-1} to 100 s^{-1} at approximately 25 °C. Enable the steady-state sensing function in the rheometer software.

2.5. Export the results table, and calculate the average value of the steady-shear viscosities.

2.6. Plot the averaged viscosity values as a function of polymer concentration.

3. Preparation of the polymer solution/nanoparticle dispersion

NOTE: To prepare a polymer solution with added nanoparticles (NPs), work inside a nano-enclosure (high-efficiency-particulate-air-filtered) hood.

3.1. Use a clean, small laboratory spatula, and weigh the required amount (*e.g.*, ~0.01 g) of dry NP powder, *e.g.*, iron oxide (Fe_3O_4) NPs, into a clean 20 mL borosilicate glass vial.

3.2. Add the desired volume (*e.g.*, nominally 10 mL) of solvent (*e.g.*, THF) using a disposable borosilicate glass pipette, and cap the borosilicate glass vial containing the NPs/solvent mixture using the provided lid.

3.3. Transfer the sample to a vortex mixer, and agitate thoroughly at room temperature at 3,000 rpm until the NPs are no longer visible at the bottom of the vial. Immediately transfer the vial with the sample to a bath sonicator to ensure full dispersion of the nanoparticles. To prevent sample from heating, sonicate the dispersion in ~30 min intervals, waiting for 2–5 min between each sonication step.

3.4. Next, working inside a chemical hood, weigh and add the desired amount (*e.g.*, ~2 g) of polymer (*e.g.*, styrene-butadiene-styrene block-co-polymer) into the NP dispersion. Seal the borosilicate glass vial with the provided lid, and mount it securely on a rotator for mixing at 70 rpm at room temperature.

3.5. Mix the polymer/NPs/solvent sample thoroughly for approximately 60 min, or until the polymer is fully dissolved.

NOTE: After mixing, the sample appears as a viscous liquid with uniformly dispersed NPs, and no large aggregates or precipitates are visible.

3.6. Finally, transfer the mixture into a DGA borosilicate glass syringe for SBS.

NOTE: It is not recommended to store the polymer NP solutions prior to SBS due to potential agglomeration or destabilization of the dispersion.

4. Solution blow spinning process (SBS)

NOTE: Suggested PPE for this process includes protective goggles, laboratory coat, and nitrile gloves; these should be donned before setting up the SBS apparatus. The setup and process should be performed inside a chemical hood. The SBS apparatus consists of a commercial airbrush unit equipped with a 0.3 mm inner nozzle (for the polymer solution) and a 1 mm head opening (for the gas), a syringe pump system, a collector, a pressurized nitrogen (N_2) gas cylinder, and an

aluminum enclosure. The inner nozzle protrudes approximately 0.5 mm from the head opening of the airbrush. Details on the SBS setup are given in **Figure 1**.

4.1. First, adjust the height and angle of the airbrush to align with the center of the selected substrate (glass microscope slide) attached to the collector, and secure it in place. Make sure the gas cylinder is properly secured to its wall mount. Then, connect the gas inlet of the airbrush to the N_2 pressurized gas cylinder.

4.2. Turn on the main valve on the gas cylinder, and slowly adjust the pressure using the pressure gauge on the gas regulator to achieve the desired flow. Ensure there is free unobstructed flow through the system, and listen carefully for any potential gas leaks at the connection points. Use a soap and water solution to further investigate potential leaks, and if necessary, apply polytetrafluoroethylene (PTFE) tape to the fittings to eliminate any leaks. When the gas flow is adjusted properly, close the main valve on the gas cylinder to stop the gas flow.

4.3. Secure the substrate on the collector using the equipped vice. Adjust the height of the collector to align perpendicular to the spray direction and pattern of the airbrush so that material will be deposited onto the substrate.

4.4. Next, slide the collector to its furthest position away from the airbrush nozzle to help with identifying the optimal working distance (separation between nozzle and substrate) in the following steps.

4.5. Working inside the chemical hood, carefully transfer the prepared polymer/NPs/solvent mixture from the borosilicate glass vial to a 10 mL DGA borosilicate glass syringe equipped with a stainless-steel needle.

4.6. Remove any air bubbles from the sample by holding the syringe with the needle pointing up, tapping the syringe gently and slowly depressing the plunger to displace any excess air. Detach the needle, and attach the syringe to the syringe-pump unit. Secure the syringe, and connect the PTFE tubing coming from the outlet of the syringe to the appropriate inlet on the airbrush.

4.7. Next, select the desired injection rate from the syringe-pump unit menu (*e.g.*, 0.5 mL/min), and slowly open the main valve on the N_2 gas cylinder to allow N_2 to flow through the airbrush. Immediately start the syringe-pump unit to dispense the polymer/NPs/solvent mixture, and initiate the spraying process.

4.8. Carefully observe the spraying pattern at the spray nozzle, and ensure that no clogs or partial clogs are present. Incrementally increase or decrease the injection rate until the solution is spraying freely.

NOTE: Very low or high injection rates are prone to clogging. The optimal injection rate is a function of the solutions viscosity and may need to be adjusted for high or low polymer solution concentrations.

4.9. Next, adjust the position of the collector to the desired working distance for the polymer/solvent system used to allow solvent evaporation by sliding it towards the airbrush until material is deposited on the substrate.

NOTE: If the collector is too close to the airbrush spray nozzle, insufficient evaporation time will result in depositing liquid polymer solution onto the substrate. If the collector is too far away, very limited or no material will be deposited onto the substrate. For poly(styrene-butadiene-styrene) solutions in THF, the appropriate working distance is between 8 cm and 12 cm.

4.10. When the desired amount of material is deposited on the substrate, stop the syringe-pump unit first, and then immediately close the main valve on the N_2 gas cylinder.

5. Analysis of SBS fiber mats by SEM

5.1. Use a sputter coater to coat the fiber mats with a conductive material such as Au/Pd to mitigate surface charging effects under the electron beam.

NOTE: A coating thickness of 4–5 nm will suffice.

5.2. Load the fiber mat samples into an SEM, and image them using an accelerating voltage of 2–5 kV and a current of 0.1–0.2 nA. Apply charge neutralization settings to counter charging effects where necessary.

5.3. Use a secondary electron detector, or a backscattered electron detector, to capture different features of the fiber materials.

5.4. Use an energy-dispersive (EDS) detector to separate the characteristic X-rays of different elements into an energy spectrum that will allow determination of the presence of iron (Fe), indicative of iron oxide NPs embedded within the polymeric fiber mats.

REPRESENTATIVE RESULTS:

In this study, non-woven fiber mats consisting of poly(styrene-butadiene-styrene) fibers in the nano- and micro-scale, were synthesized with and without the presence of iron oxide NPs. To form fibers, the SBS parameters must be carefully selected for the polymer/solvent system used. The molar mass of the dissolved polymer and the solution concentration are critical in controlling the morphology of the structures produced by the SBS process. In this study, a poly(styrene-butadiene-styrene) block-co-polymer (styrene 30 wt. %) was used with a molar mass of approximately 185,000 g/mol and a density of 0.94 g/mL at 25 °C. Multiple studies have examined the effects of polymer molar mass, demonstrating that a higher molar mass favors chain entanglement in solution and drastically increases its viscosity, resulting in fiber formation via the SBS technique[21]. In addition, previous studies have shown that polymer concentrations in a good solvent (as defined by Flory[22]) well above the critical overlap concentration ($c >> c^*$), also known as the entanglement concentration ($C_e \sim 10c^*$), will result in fiber formation with minor or no

bead formation[21,23].

This phenomenon is again governed by the interactions between the entangled polymer chains in solution. Entanglement of the molecules in solution above the c* exponentially increases the viscosity of the solution, therefore overcoming the inertial capillary forces and suppressing the breakup of the polymer jet. Destabilization of the polymer jet after shearing off the polymer solution stream from the nozzle will lead to undesirable "bead" formation if the selected concentration for the SBS experiment is too low. In this study, the critical overlap concentration of the poly(styrene-butadiene-styrene) block-co-polymer in THF was first estimated using the following equation for random polymer coils in a good solvent[24]:

$$c^* \approx 3M_w / (4\pi N_A {R_g}^3) \quad (1)$$

In equation (1) above, N_A, M_w, and R_g are the Avogadro's number, the molar mass of the polymer, and the radius of gyration of the polymer, respectively. This equation estimated the c* of the polymer in solution to be ~8.96 mg/mL. Eight polymer solutions were prepared with different concentrations and their viscosity studied as a function of concentration. For most polymers, the behavior of their solution's viscosity in a good solvent is linear only at low concentrations.

As polymer concentration increases, the viscosity rises exponentially, and the critical overlap concentration corresponds to the value at which the dissolved polymer coils start to overlap each other and cause entanglement. At that critical concentration, a polymer solution transitions from a dilute to a semi-dilute regime[25]. The results of the polymer solution's viscosity as a function concentration are shown in **Figure 2**, and the value of the experimentally estimated c* is ~9.28 mg/mL. The calculated and experimentally predicted values of c*are similar, which is ~10 mg/mL. Therefore, polymer concentration values greater than 10c* (c ≥ 100 mg/mL) were selected to use for the SBS process, to be in the entanglement concentration regime[23]. At these higher concentrations, the SBS apparatus is capable of consistently producing non-woven fibers with desired diameters and morphology. **Figure 3** shows the structure of the developed fiber mats and the morphology of the fibers at a polymer concentration of ~200 mg/mL, N_2 gas pressure of approximately 207 kPa, a working distance of nominally 8 cm, and a polymer solution injection rate of ~0.5 mL/min.

The electron micrograph in **Figure 3A** shows the morphology of the non-woven fiber mat at low magnification. The fiber mat sample consists of primarily individual and cylindrically shaped fibers with minimal polymer beads or polymer welding present. At higher magnification (**Figure 3B**), it is apparent that the fibers formed are smooth and round, with very similar diameters in the nano scale (diameter range from 100 nm to 600 nm). Individual fibers, as well as some bundle of fibers consisting of 2, 3, and sometimes 4 individual fibers are observed. Finally, the higher magnification images confirm the absence of polymer beads ("beads-on-a-string") or polymer welding under these SBS conditions. To better understand this specific polymer/solvent system and the effect of polymer concentration on the fiber mats produced, the structure and morphology of fiber mat samples sprayed at various concentrations were examined. Significant differences in the fiber mats produced were observed as the polymer concentration increased from approximately 100 mg/mL to 120 mg/mL, 150 mg/mL, and 200 mg/mL, respectively, as seen

in **Figure 4**. The SEM micrographs show a clear transition from fibers that exhibit the undesired "beads-on-a-string" morphology with numerous bundles of fibers present at lower concentrations, near the critical overlap concentration (c* ~10 mg/mL), to the formation of pristine and morphologically smooth fibers at concentrations well above c* (*e.g.*, 200 mg/mL).

Furthermore, as mentioned previously, the gas pressure is another process variable that can influence the morphology and diameter of the produced fibers, although to a much lesser extent than polymer molar mass and concentration. **Figure 5** demonstrates the effects of gas pressure, indicating the presence of fibers with decreasing diameter as gas pressure increased from ~138 kPa to ~345 kPa; however, the presence of large polymer beads and welded fibers also increased. Prior work has also demonstrated that very high gas pressures will induce undesirable fiber and polymer welding[17,19]. This effect could be a result of a more significant decrease in temperature at the spray nozzle when higher gas flow rates are used, due to Joule expansion of the gas. The temperature decrease is proportional to the volumetric expansion of the gas, which in turn, can cause poor solvent evaporation and fiber welding[17,19,26]. In the current study, based on various SBS parameters and SEM imaging, the optimal polymer concentration and carrier gas pressure for the polymer/solvent system were determined to be 200 mg/mL and 207 kPa.

This combination can consistently produce pristine, smooth, individual fibers in the nano scale (diameter of ~100 nm to 600 nm) without the presence of beads or fiber welding, as shown in **Figure 3**. It is useful to note that the nitrogen gas was fed to the SBS sprayer through a PTFE tube with an inner diameter of 0.238 cm and length of 2.134 m. At the optimal nitrogen pressure of 207 kPa and approximately 20 °C, the N_2 gas density is 0.00215 kg/L, its dynamic viscosity is 1.76 x 10^{-5} Pa·s, and its approximate velocity is 0.871 m/s with a Reynold's number of 147, indicating a laminar flow. After identifying the best conditions for the SBS parameters in this spray setup for poly(styrene-butadiene-styrene) in THF, the capability of the technique to produce polymer elastomer nanocomposite fiber mats was investigated by dispensing iron oxide NPs in the polymer solution at a mass fraction of χ_{np} = 0.001. This mass fraction was determined to be the highest attainable before destabilization of the NP dispersion was observed. As the NP dispersions were not stable above χ_{np} = 0.001, no dispersions were sprayed at NP mass fractions above this value. Nanoparticle agglomeration phenomena are to be expected, which can later affect the quality of the fibers produced (irregular fiber morphology and diameters) and result in a non-uniform dispersion of the NPs within the fiber material.

It is important to note that after sonication, the iron oxide NP/polymer dispersions at mass fractions equal to 0.001 were stable for approximately 2 hours; therefore, it is recommended to use them immediately after mixing for optimal results. If the dispersions are left unmixed for more than a few hours, it is recommended to sonicate the samples again before beginning SBS. The NPs used in this study, in the form of dry powder, were coated by the manufacturer with silicon oil, which renders them easily dispersible in various organic solvents, including THF. The fiber mats produced were evaluated using backscattered electron (BSE) analysis and EDS in an SEM, and the results demonstrate the presence of iron oxide NPs within the polymer fibers. A representative electron micrograph collected via a BSE detector is shown in **Figure 6A**. The iron oxide particles (circled in red) can be easily identified in the fibers due to their brighter contrast

from the surrounding polymeric fiber material using a BSE detector, as iron is a much heavier element than carbon. In **Figure 6C**, EDS elemental analysis of the same sample indicates the present of iron (marked red) at the brighter contrast locations where the iron oxide NPs reside, further validating their presence within the fibers. It is worth noting that the structure and morphology of the fiber mats were not significantly affected by the presence of the iron oxide NPs.

FIGURE AND TABLE LEGENDS:

Figure 1: The solution blow spinning apparatus. (**A**) The apparatus comprises a syringe pump system, an airbrush setup, a collector, an aluminum enclosure, and a nitrogen gas cylinder (not shown); details on the (**B**) airbrush setup and (**C**) substrate holder are shown.

Figure 2: Viscosity of polymer solutions as a function of polymer concentration. The critical overlap concentration (c*) is estimated by the onset of the power law behavior of the viscosity as indicated by the arrow in the graph.

Figure 3: Scanning electron microscopy (SEM) images of poly(styrene-butadiene-styrene) fibers formed via the solution blow spinning (SBS) apparatus. (**A**) Low-magnification image, and (**B**) higher-magnification image of the same sample. Scale bar for **A** = 1 mm; scale bar for **B** = 40 µm.

Figure 4: SEM micrographs of poly(styrene-butadiene-styrene) solutions sprayed using the SBS apparatus at increasing polymer concentration in solution. Polymer concentration increases from left to right. Scale bars = 40 µm. Abbreviations: SEM = scanning electron microscopy; SBS = solution blow spinning.

Figure 5: SEM micrographs of poly(styrene-butadiene-styrene) solutions sprayed using the SBS apparatus. (**A**) High gas pressure of 345 kPa and (**B**) low gas pressure of 138 KPa. Scale bars = 50 µm.

Figure 6: Backscattered electron micrograph of solution blow spun poly(styrene-butadiene-styrene) fibers. (**A**) Infused iron oxide (Fe_3O_4) nanoparticles circled in red; scale bar = 10 µm. (**B**) Enlargement of the yellow highlighted area at the same magnification. (**C**) Energy-dispersive X-ray spectroscopy of the enlarged area, indicating the presence of iron (elemental analysis; Fe stained red) within the fibers. Scale bars (**B,C**) = 4 µm.

DISCUSSION:

The method described herein provides a protocol for producing polymer elastomer nanocomposite fiber mats via a relatively new technique—SBS. This technique allows the fabrication of fibers in the nanoscale and has several advantages over other well-established techniques, such as the electrospinning process, as it can be carried out under atmospheric pressure and room temperature[27]. Furthermore, SBS is not highly susceptible to local environmental changes (temperature or humidity) and does not require harsh or toxic chemicals, nor a high voltage gradient, which is beneficial when working with biological systems[17,19,28,29]. Finally, the solution deposition rates of the SBS process are roughly 10 times faster than those of

electrospinning, covering larger areas in less time and promising ease of process scale-up[14,17].

To obtain desirable results from this technique and the protocol described herein, the operator needs to carefully select the materials and have control over certain important parameters, such as the polymer molar mass and concentration, as well as the carrier gas pressure. The selection of the desired polymer will dictate the solvent that should be used. The solvent needs to be volatile at ambient conditions and must be a good solvent for the selected polymer to be dissolved at concentrations equal or greater than the c*, which can be achieved by examining the Hildebrand solubility parameters (δ).

In this study, it was recommended to use a solvent with solubility parameters between 7.7 and 9.4 for the poly(styrene-butadiene-styrene) block-co-polymer used. Therefore, THF was as a solvent with a Hildebrand solubility parameter of $\delta = 9.1$[30]. Next, the molar mass of the polymer (~180,000 g/mol) was judiciously selected to be high enough to promote polymer chain entanglements and achieve solutions with sufficiently high viscosities that were previously shown to favor fiber formation via the SBS technique[21]. The structure and morphology of the produced fibers vary not only with increasing molar mass, but also with polymer concentration.

The results of this study have shown that concentrations well above the critical overlap concentration ($c >> c^*$) result in fibers with optimal size and morphology, which is also well supported by the literature[14,17,21]. Then, the effect of the carrier gas pressure was investigated; extremely low or high values were found to negatively impact the fiber morphology. Smaller fiber diameters were observed with increasing gas pressure values, along with the formation of fiber welding at very high pressures. Therefore, gas pressures of ~207 kPa are desirable for this polymer/solvent system and this SBS setup. These changes in the morphology of the produced fibers as a result of the gas pressure were also observed in a study by Medeiros et al.[14].

Finally, other parameters including the working distance, polymer solution injection rate, and spraying time were kept constant at values that allowed proper solvent evaporation, no clogging issues at the spray nozzle, and same amounts of deposited material, respectively. Ultimately, fibrous materials developed via the SBS process have numerous applications in various field including medical products, air filters, protective equipment, sensors, optical electronics, and catalysts[14,19,20]. Thus, the ultimate goal of this research is to use the SBS technique described herein to create tunable polymer elastomer nanocomposites, and apply them to advance various fields, such as the personal protective equipment field, which involve the use of novel multifunctional materials.

ACKNOWLEDGMENTS:

The authors would like to acknowledge Mr. Dwight D. Barry for his important contributions for fabrication of the solution blow spinning apparatus. Zois Tsinas and Ran Tao would like to acknowledge funding from the National Institute of Standards and Technology under Awards # 70NANB20H007 and # 70NANB15H112, respectively.

DISCLOSURES:

The full description of the procedures used in this paper requires the identification of certain commercial products and their suppliers. The inclusion of such information should in no way be construed as indicating that such products or suppliers are endorsed by NIST or are recommended by NIST or that they are necessarily the best materials, instruments, software or suppliers for the purposes described.

REFERENCES:

1 Lee, B. L. et al. Penetration failure mechanisms of armor-grade fiber composites under impact. *Journal of Composite Materials.* **35** (18), 1605–1633 (2001).

2 Prevorsek, D. C., Kwon, Y. D., Chin, H. B. Analysis of the temperature rise in the projectile and extended chain polyethylene fiber composite armor during ballistic impact and penetration. *Polymer Engineering and Science.* **34** (2), 141–152 (1994).

3 Park, A. D., Park, D., Park, A. J. U.S. Patent No. 7,148,162 (2006).

4 Park, A. D. U.S. Patent No. 5,437,905 (1995).

5 Harpell, G. A., Prevorsek, D. C., Li, H. L. Flexible multi-layered armor. Patent No. WO/1989/001125 (1989).

6 Cena, C. et al. BSCCO superconductor micro/nanofibers produced by solution blow-spinning technique. *Ceramics International.* **43** (10), 7663–7667 (2017).

7 Miller, C. L., Stafford, G., Sigmon, N., Gilmore, J. A. Conductive nonwoven carbon nanotube-PLA composite nanofibers towards wound sensors via solution blow spinning. *IEEE Transactions on Nanobioscience.* **18** (2), 244–247 (2019).

8 Iorio, M. et al. Conformational changes on PMMA induced by the presence of TiO 2 nanoparticles and the processing by Solution Blow Spinning. *Colloid and Polymer Science.* **296** (3), 461–469 (2018).

9 Martínez-Sanz, M. et al. Antimicrobial poly (lactic acid)-based nanofibres developed by solution blow spinning. *Journal of Nanoscience and Nanotechnology.* **15** (1), 616–627 (2015).

10 Wang, H. et al. Highly flexible indium tin oxide nanofiber transparent electrodes by blow spinning. *ACS Applied Materials and Interfaces.* **8** (48), 32661–32666 (2016).

11 Greenhalgh, R. D. et al. Hybrid sol–gel inorganic/gelatin porous fibres via solution blow spinning. *Journal of Materials Science.* **52** (15), 9066–9081 (2017).

12 Gonzalez-Abrego, M. et al. Mesoporous titania nanofibers by solution blow spinning. *Journal of Sol-Gel Science and Technology.* **81** (2), 468–474 (2017).

13 Oliveira, J. E., Zucolotto, V., Mattoso, L. H., Medeiros, E. S. Multi-walled carbon nanotubes and poly (lactic acid) nanocomposite fibrous membranes prepared by solution blow spinning. *Journal of Nanoscience and Nanotechnology.* **12** (3), 2733–2741 (2012).

14 Medeiros, E. S., Glenn, G. M., Klamczynski, A. P., Orts, W. J., Mattoso, L. H. Solution blow spinning: A new method to produce micro-and nanofibers from polymer solutions. *Journal of Applied Polymer Science.* **113** (4), 2322–2330 (2009).

15 Vasireddi, R. et al. Solution blow spinning of polymer/nanocomposite micro-/nanofibers with tunable diameters and morphologies using a gas dynamic virtual nozzle. *Scientific Reports.* **9** (1), 1–10 (2019).

16 Tutak, W. et al. The support of bone marrow stromal cell differentiation by airbrushed nanofiber scaffolds. *Biomaterials.* **34** (10), 2389–2398 (2013).

17 Daristotle, J. L., Behrens, A. M., Sandler, A. D., Kofinas, P. A review of the fundamental

principles and applications of solution blow spinning. *ACS Applied Materials and Interfaces.* **8** (51), 34951–34963 (2016).
18 Hofmann, E. et al. Microfluidic nozzle device for ultrafine fiber solution blow spinning with precise diameter control. *Lab on a Chip.* **18** (15), 2225–2234 (2018).
19 Behrens, A. M. et al. In situ deposition of PLGA nanofibers via solution blow spinning. *ACS Macro Letters.* **3** (3), 249–254 (2014).
20 Vural, M., Behrens, A. M., Ayyub, O. B., Ayoub, J. J., Kofinas, P. Sprayable elastic conductors based on block copolymer silver nanoparticle composites. *Acs Nano.* **9** (1), 336–344 (2015).
21 Srinivasan, S., Chhatre, S. S., Mabry, J. M., Cohen, R. E., McKinley, G. H. Solution spraying of poly (methyl methacrylate) blends to fabricate microtextured, superoleophobic surfaces. *Polymer.* **52** (14), 3209–3218 (2011).
22 Flory, P. J. *Principles of polymer chemistry*. Cornell University Press (1953).
23 Palangetic, L. et al. Dispersity and spinnability: Why highly polydisperse polymer solutions are desirable for electrospinning. *Polymer.* **55** (19), 4920–4931 (2014).
24 Ying, Q., Chu, B. Overlap concentration of macromolecules in solution. *Macromolecules.* **20** (2), 362–366 (1987).
25 Haro-Pérez, C., Andablo-Reyes, E., Díaz-Leyva, P., Arauz-Lara, J. L. Microrheology of viscoelastic fluids containing light-scattering inclusions. *Physical Review E.* **75** (4), 041505 (2007).
26 Thiele, J. et al. Early development drug formulation on a chip: Fabrication of nanoparticles using a microfluidic spray dryer. *Lab on a Chip.* **11** (14), 2362–2368 (2011).
27 Zhao, J., Xiong, W., Yu, N., Yang, X. Continuous jetting of alginate microfiber in atmosphere based on a microfluidic chip. *Micromachines.* **8** (1), 8 (2017).
28 Jun, Y., Kang, E., Chae, S., Lee, S.H. Microfluidic spinning of micro-and nano-scale fibers for tissue engineering. *Lab on a Chip.* **14** (13), 2145–2160 (2014).
29 Weng, B., Xu, F., Salinas, A., Lozano, K. Mass production of carbon nanotube reinforced poly (methyl methacrylate) nonwoven nanofiber mats. *Carbon.* **75**, 217–226 (2014).
30 Barton, A. F. Solubility parameters. *Chemical Reviews.* **75** (6), 731–753 (1975).

Figure 1

Click here to access/download;Figure;Figure 1_ppt v.03.tif

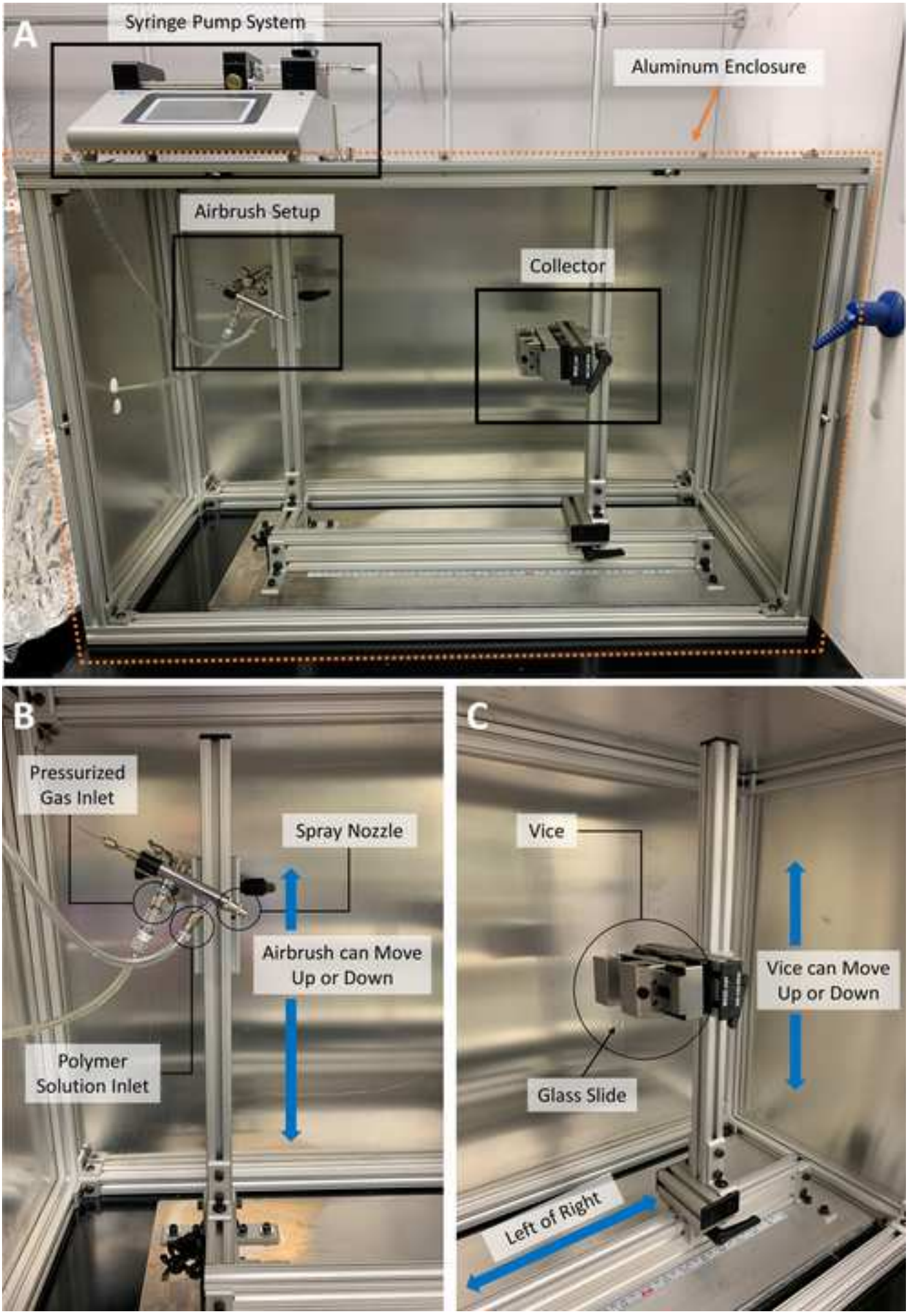

Figure 2

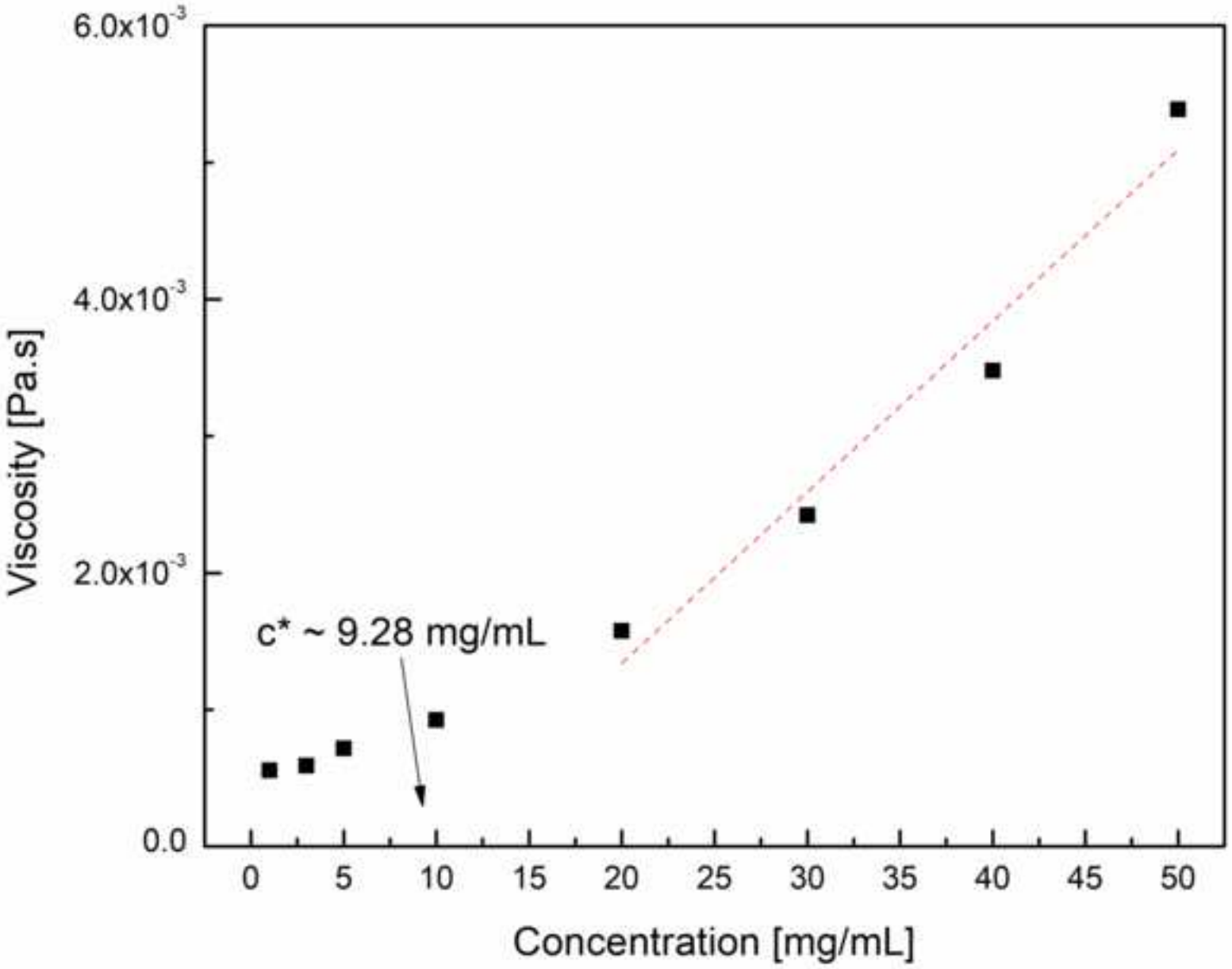

Figure 3

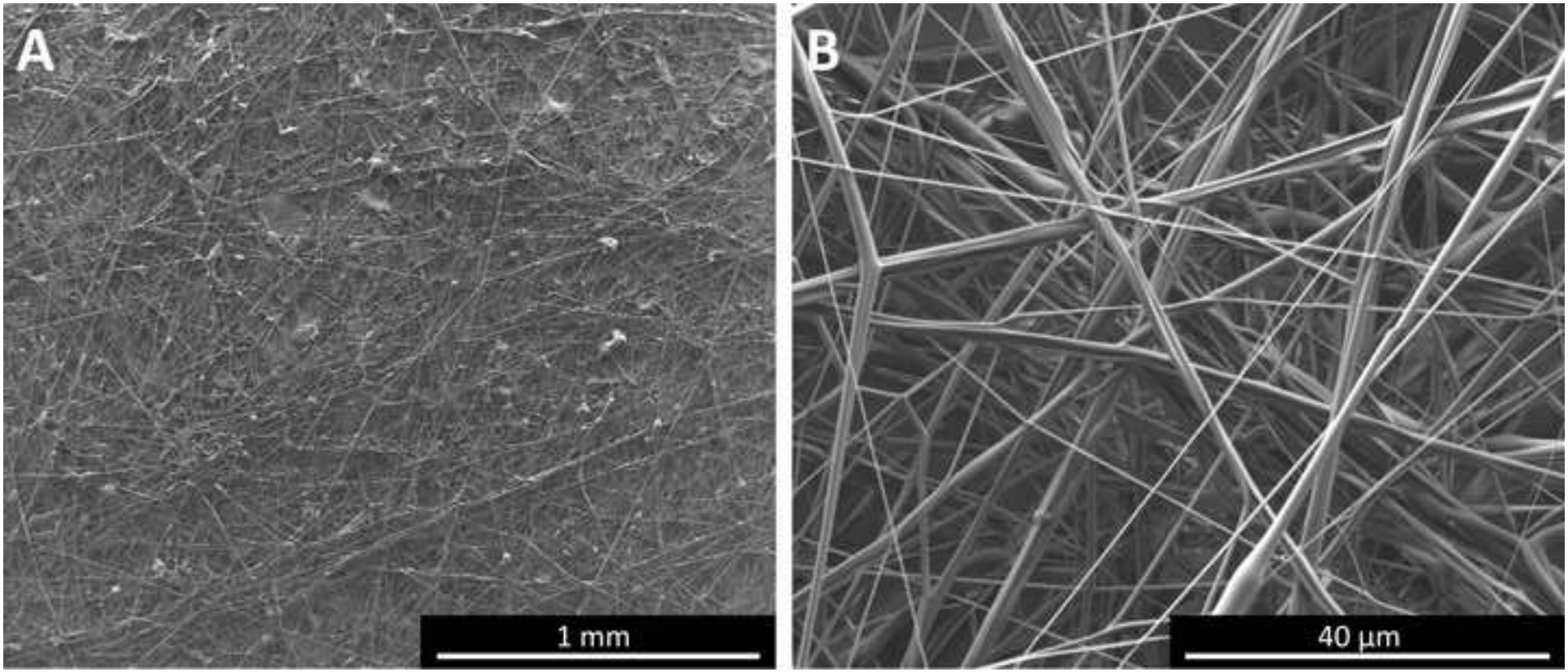

Figure 4

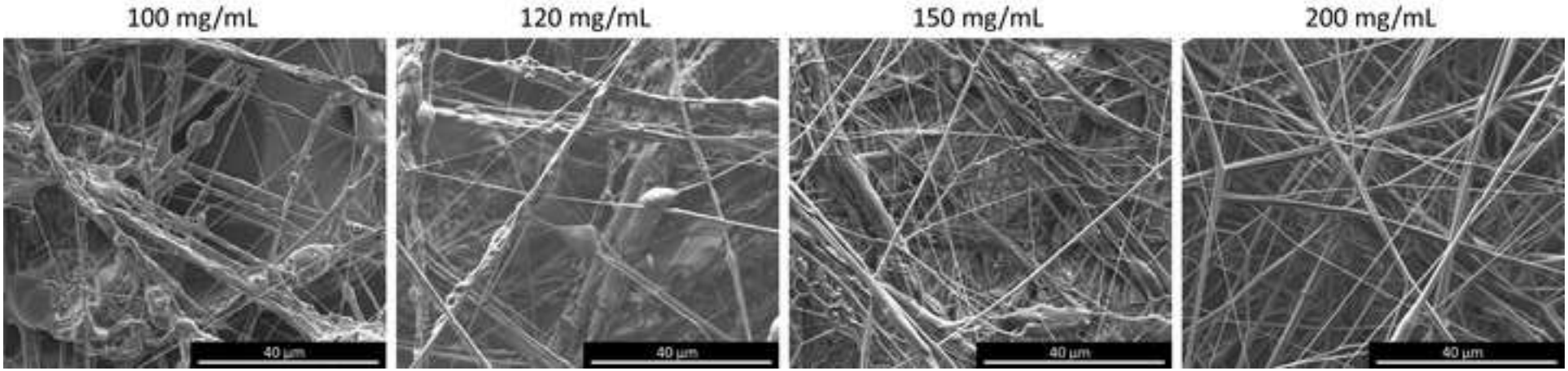

Figure 5

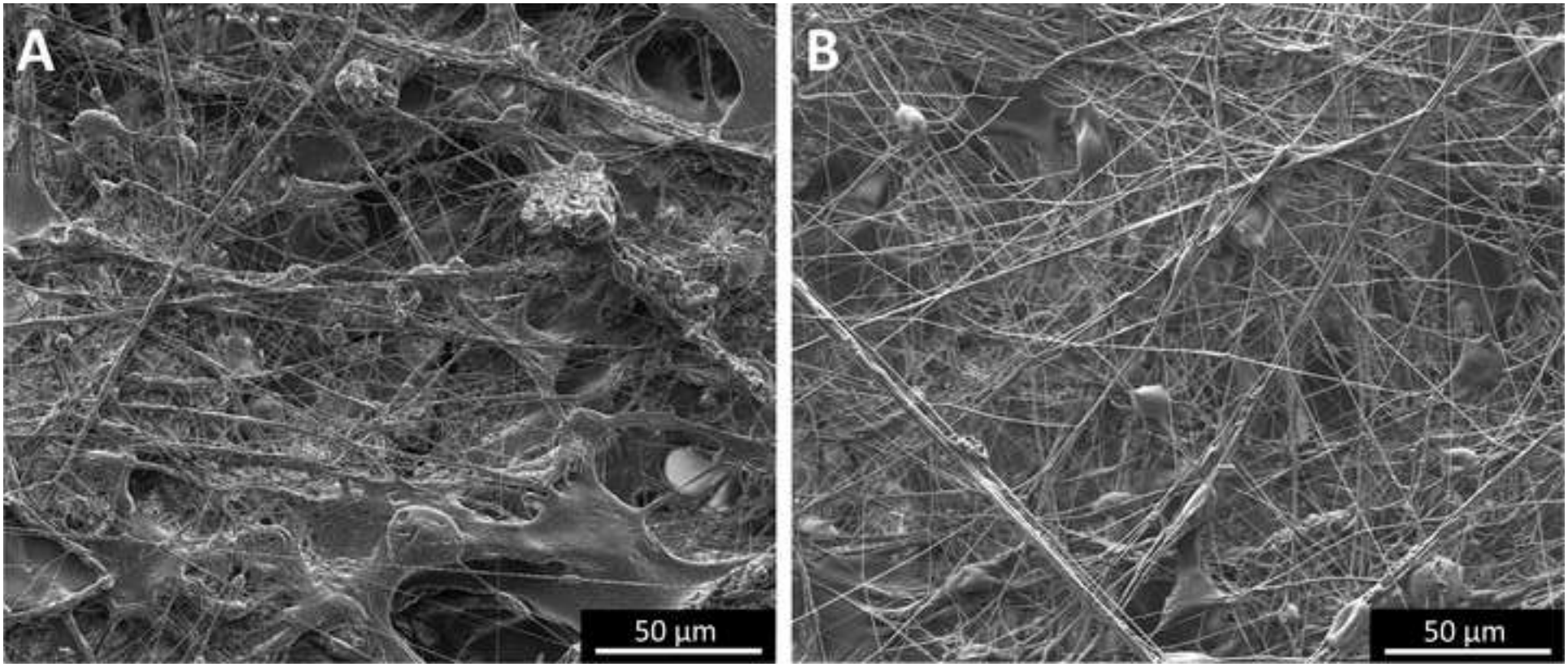

Figure 6

Click here to access/download;Figure;Figure 6_ppt v.01.tif

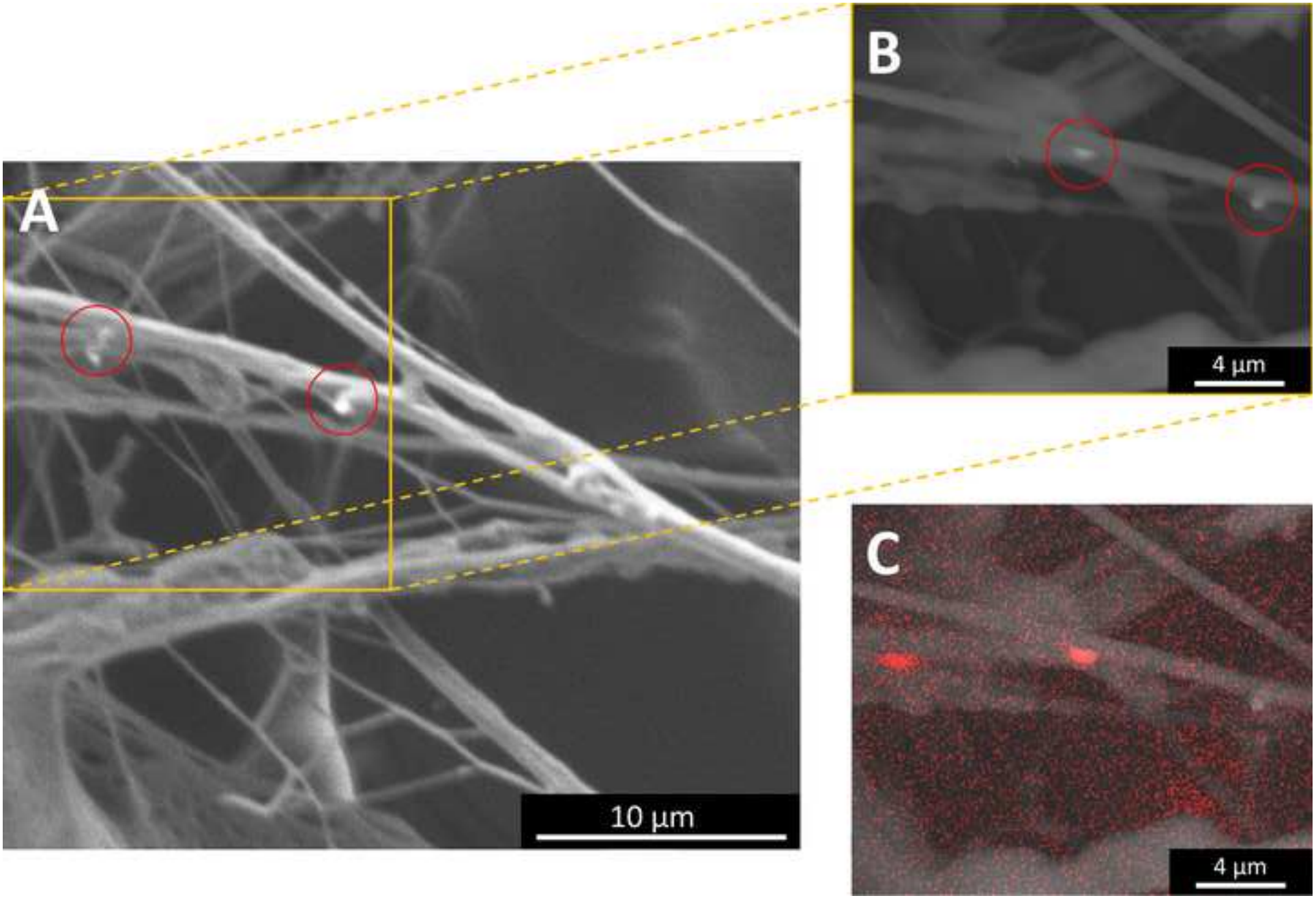

Table of Materials

Click here to access/download;Table of Materials;JoVE_Table_of_Materials_v.03.xlsx

Name of Material/Equipment	Company	Catalog Number
45 MM Toolmaker Vise	Tormach Inc.	32547
ARES-G2 Rheometer	TA Instruments	401000.501
Branson Ultrasonics M Series - Ultrasonic Cleaning Bath	Fisher Scientific	15-336-100
Cadence Science Micro-Mate Interchangeable Syringe	Fisher Scientific	14-825-2A
Chemical hood	Any company	
Corning - Disposable Pasteur Glass Pipette	Sigma Aldrich	CLS7095D5X-200EA
DWK Life Sciences Wheaton - Glass Scintillation Vial	Fisher Scientific	03-341-25G
FEI Quanta 200 Scanning Electron Microscope (SEM)	FEI	
Iron Oxide Nanopowder/Nanoparticles	US Research Nanomaterials, inc.	US3320
KD Scientific Legato 100 Single-Syringe Pump	Sigma Aldrich	Z401358-1EA
Master Airbrush - Model S68	TCP Global	MAS S68
Mettler Toledo AB265-S/FACT Scale	Cole-Parmer Scientific	EW-11333-14
N2 Gas Regulator	Any company	
Nanoenclosure	Any company	
Optical Microscopy Glass Slides	Fisher Scientific	12-550-A3
OSP Slotted Bob, 33 mm	TA Instruments	402796.902
OSP Slotted Double Gap Cup, 34 mm	TA Instruments	402782.901
Oxford BenchMate Digital Vortex Mixer	Pipette	VM-D
Oxford Benchmate Tube Roller	Pipette	OTR-24DR
Polystyrene-block-polybutadiene-block-polystyrene	Sigma Aldrich	432490-1KG
SEM Pin Stub Specimen Mount	Ted Pella Inc.	16119
Spatula	VWR	82027-532
Tetrahydrofuran (THF)	Fisher Scientific	T425-1
TRIOS	TA Instruments	v4.3.1.39215

Comments/Description
To secure substrate onto the collector
Rheometer
To disperse nanoparticles
Glass Syringe 5mL in 1/5mL, Luer Lock Tip

Non-Sterile
20 mL with cap
For imaging samples
Fe3O4, 98%, 20-3- nm, Silicon oil Coated
Single syringe infusion pump
Nozzle/needle diameter: 0.35 mm
For weighing polymer and Nanoparticles

Used as a substrate for fiber mat deposition
Bob, upper geometry
Double wall cup, lower geometry
Rated up to 4,200 rpm, for mixing solutions
Sample mixer/rotator
styrene 30 wt. %, Mw ~ 185,000 g/mol
18 mm diameter x 8 mm height
To load test materials
solvent, HPLC grade
Rheometer software

Dear Dr. Nguyen,
Please find below our responses to the reviewers regarding JoVE submission JoVE62283, manuscript "Protocol for Solution Blow Spinning of Polymeric Nano-Composite Fibers for Personal Protective Equipment". Thank you very much for your time and consideration.
Sincerely,

Amanda Forster, on behalf of the coauthors

Editorial Comments:

Comment 1:

Please take this opportunity to thoroughly proofread the manuscript to ensure that there are no spelling or grammar issues.

Author's Response to Comment 1:
We would like to thank the editors for this comment. A careful and thorough check was completed to eliminate all possible spelling or grammar issues.

Comment 2:

Please ensure that all text in the protocol section is written in the imperative tense as if telling someone how to do the technique (e.g., "Do this," "Ensure that," etc.). The actions should be described in the imperative tense in complete sentences wherever possible. Avoid usage of phrases such as "could be," "should be," and "would be" throughout the Protocol. E.g. Line 122: "Transfer the solution to a syringe.." instead of "The solution is now ready…".

Author's Response to Comment 2:
Thank you very much for bringing this issue to our attention. The protocol section was proofread thoroughly and every sentence is written in the imperative tense. Also, phrases such as "could be", "should be", and "would be" are eliminated from the protocol.

Comment 3:

Any text that cannot be written in the imperative tense may be added as a "Note." Please consider adding the following as Caution/Note instead of a protocol step: E.g. Line 104-106, Line 124-126, Line 162-163, Line 189-191 (Caution), Line 191 – 194 (note).

Author's Response to Comment 3:
We would like to thank the editors for the recommendations above. We have addressed the issues as recommended and the text in the aforementioned lines was removed from the protocol and added as "Caution" or "Note".

Comment 4:

Please remove the "&" in the references, to follow the JoVE reference format: [Lastname, F.I., LastName, F.I., LastName, F.I. Article Title. Source. Volume (Issue), FirstPage – LastPage (YEAR).] For more than 6 authors, list only the first author then et al.

Author's Response to Comment 4:
Thank you for pointing this out. All the references were corrected as suggested.

Comment 5:

Lines 119, 170, 177: At what speed, temperature should the solution be agitated/rotated?

Author's Response to Comment 5:
Thank you for bringing this matter to our attention.
Text in line 119 was modified to highlight the speed and temperatures used for mixing of the solutions.

Comment 6:

Please specify the grade of glass used e.g. for vials and syringes.

Author's Response to Comment 6:
We would like to thank the editors for this question. All the glass vials used in this work are "borosilicate glass vials", the disposable glass pipets used to transfer the solution are "high-quality disposable borosilicate pipets", and the syringe used for solution blow spinning is a "dissolved gas analysis (DGA) borosilicate syringe". The information is added in the manuscript where relevant.

Comment 7:

Line 204: "..apply PTFE tape.." instead of "..add PTFE tape".

Author's Response to Comment 7:
*Thank you for this suggestion. We have modified this phrase so that the sentence reads as suggested: "if necessary, **apply** polytetrafluoroethylene (PTFE) tape to the fittings to eliminate any leaks".*

Comment 8:

Line 247: How should the coat be applied? With what device?

Author's Response to Comment 8:
*Thank you for pointing this out. A gold/palladium sputter coater was used to coat the fiber samples for SEM analysis. The text in the manuscript has been changed accordingly: "**Use a***

sputter coater to *coat the fiber mats with a conductive material such as Au/Pd to mitigate surface charging effects under the electron beam. A coating thickness of 4 nm to 5 nm will suffice".*

Reviewer #2

Reviewer Comment 1:
p3 l68 - Another recent solution blow spinning article can be found here:
https://doi.org/10.1039/C8LC00304A

Author's Response to Reviewer Comment 1:
We thank the reviewer for recommending this very useful article to us. We have cited this article in our manuscript as suggested.

Reviewer Comment 2:
p8 263ff. The manuscript should contain the block length ratio and monomer numbers of the poly(styrene-butadiene-styrene) somewhere. I am also missing Mn and its polydispersity index of the three blocks.

Author's Response to Reviewer Comment 10:
Thank you for bringing this issue to our attention. The poly(styrene-butadiene-styrene) block-co-polymer used in this study had a styrene content of 30 wt. %, a molar mass of ~185,000 g/mol, and a density of 0.94 g/mL at 25 °C. The molar mass characterization was performed by the vendor via viscosity/IR measurements. Unfortunately, no information about the polydispersity index or the molar mass of the block chains was provided. The exact polymer used (vendor, catalog number, batch, etc.) in this study can be found in the "Table of Materials" submitted along with the manuscript. Due to current COVID-19 restrictions and the lack of available equipment in our laboratory, we are not currently able to perform additional GPC experiments to verify the information from the manufacturer. The information that we do have, as stated above, was added to the manuscript in the section as suggested by the reviewer.

Reviewer Comment 3:
p10 l317ff. - When discussing the influence of the gas pressure, it would be good to know the dimensions of the spray device. What Reynolds numbers is the gas operated at? How do the fiber spinning outcomes vary with the dimensions of the sprayer geometry? (e.g. gas channel diameter, inlet diameters, inner tube wall thickness, of liquid inlet position within the gas stream (how deep inside or how far sticking out?). Such details should be described for the reader to be able to buy the right parts and replicate the results.

Author's Response to Reviewer Comment 3a:
We would like to thank the reviewer for bringing these issues for discussion to our attention.

The optimal nitrogen gas pressure for this work was identified to be 207 kPa, as mentioned in the manuscript. At that pressure and ~20 °C the nitrogen gas has a density of 0.00215 kg/L, dynamic viscosity of 1.76 x 10^{-5} Pa·s, velocity of 0.871 m/s and a Reynold's number of 147. This is a low Reynold's number for the flow of nitrogen gas in the gas channel/tube (inner diameter of 0.238 cm & length of 2.134 m) feeding the sprayer, indicative of a laminar flow. We have added the following sentence to address the above in the manuscript, line 328: "It is useful to note that the nitrogen gas was fed to the solution blow spinning sprayer through a PTFE tube with an inner diameter of 0.238 cm and length of 2.134 m. At the optimal nitrogen pressure of 207 kPa and approximately 20 °C, the N_2 gas density is 0.00215 kg/L, its dynamic viscosity is 1.76 x 10^{-5} Pa·s, and its approximate velocity is 0.871 m/s with a Reynold's number of 147, indicating a laminar flow".

In this study we used a commercially available airbrush unit. The manufacturer and model of the airbrush can be found in the "Table of Materials" document submitted along with the manuscript. No alterations/modifications were made to the unit. This airbrush unit was equipped by the manufacturer with a 0.35 mm inner nozzle (for the solution) and a corresponding head with an opening of 1 mm in diameter (for the gas). The inner nozzle protrudes ("sticks out") approximately 0.5 mm from the 1 mm opening of the head. We have added the information above in the "Solution Blow Spinning Process (SBS)" section of the manuscript, line 191: "The SBS apparatus consists of a commercial airbrush unit equipped with a 0.3 mm inner nozzle (for the polymer solution) and a 1mm head opening (for the gas), a syringe pump system, a collector, a pressurized nitrogen (N_2) gas cylinder, and an aluminum enclosure. Also, the inner nozzle protrudes approximately 0.5 mm from the head opening of the airbrush. Details on the SBS setup are given in Figure 1".

Reviewer Comment 4:

p10 l330ff. - What is the w/w% of NP and polymer? It should be mentioned here and not force the reader to reconstruct it from p6 l 165. The incorporation of NPs looks very scarce. What is the range of compatible NP filling ratios? How high can you go without NP agglomeration and stable spinning? After what time did the NP-containing spinning solutions become unusable/agglomerated? What was the influence of the mentioned oil on the polymer fiber quality and porosity?

Author's Response to Reviewer Comment 4:

Thank you very much for bringing this issue to our attention. We have addressed the reviewer's comment by adding the following discussion in our manuscript, "Representative Results" section line 332 and below: "…elastomer nanocomposite fiber mats by dispensing iron oxide NPs in the polymer solution at a mass fraction of, χ_{np} = 0.001. This mass fraction was determined to be the highest attainable before destabilization of the NP dispersion was observed. Since the NP dispersions where not stable above χ_{np} = 0.001, no dispersions where sprayed at NP mass fractions above this value. Nanoparticle agglomeration phenomena are to be expected, which can later affect the quality of the fibers produced (irregular fiber morphology and diameters) and result in a non-uniform dispersion of the NPs within the fiber material. It is important to note that after sonication, the iron oxide NP/polymer dispersions at mass fractions equal to 0.001 were stable

for approximately 2 hours, therefore it is recommended to use them immediately after mixing for optimal results. If the dispersions are left unmixed for more than a few hours it is recommended to sonicate the samples again before beginning solution blow spinning. The NPs used in this study, in thea form of dry powder, were coated by the manufacturer with silicon oil, which renders them easily dispersible in various organic solvents, including THF".

Reviewer Comment 5:

p12 l394 - The mentioned fiber welding at higher pressures could come from the faster velocity and resulting decrease in drying time. This can potentially be compensated for by increasing the distance. Maybe this dynamic could be discussed here in the manuscript? A similar principle has been demonstrated for a spray dryer in:
https://pubs.rsc.org/en/content/articlelanding/2011/lc/c1lc20298g/unauth#!divAbstract

Author's Response to Reviewer Comment 5:

We thank the reviewer for bringing this point to our attention. The effect of the gas pressure and the fiber welding phenomenon was discussed in our manuscript in the "Representative Results" section beginning of line 314. We have also cited the published work suggested by the reviewer in our discussion. The discussion is copied here for convenience:

"Furthermore, as mentioned previously, the gas pressure is another process variable that can have an effect on the morphology and diameter of the produced fibers, although to a much lesser extent than polymer molar mass and concentration. Figure 5 demonstrates the effects of gas pressure indicating the presence of fibers with decreasing diameter as gas pressure increases from about 138 kPa to about 345 kPa, however the presence of large polymer beads and welded fibers is also increased. Prior work has also demonstrated that very high gas pressures will induce undesirable fiber and polymer welding[17,19]. This effect could be a result of a more significant decrease in temperature at the spray nozzle when higher gas flow rates are used, due to Joule expansion of the gas. The temperature decrease is proportional to the volumetric expansion of the gas, which in turn can cause poor solvent evaporation and fiber welding[17,19,26]."

As the reviewer suggested in his comment, we could compensate for the poor solvent evaporation at higher gas pressures by increasing the working distance, but we have found that no added benefits were obtained and we recommend using lower gas pressures for optimal results (homogeneous fiber deposition, even fiber coverage on the substrate, best fiber morphology, etc.).